ICMA 2021
1st International Conference on Micromachines and Applications
15–30 APRIL 2021 | ONLINE
micromachines
MDPI

Droplet formation in a cross-junction with non-Newtonian dispersed phase

Maryam Fatehifar [1,*], Alistair Revell [1], and Masoud Jabbari [1]

Department of Mechanical, Aerospace and Civil Engineering, University of Manchester, Manchester, M13 9PL, UK

* Corresponding author: maryam.fatehifar@manchester.ac.uk

MANCHESTER 1824
The University of Manchester

Abstract

Microfluidics enables generating series of isolated droplets for high-throughput screening. As many biological/chemical solutions are of shear thinning non-Newtonian nature [1,2], we studied non-Newtonian droplet generation to improve the reliability of simulation results in real-life assays. We considered non-Newtonian power-law behaviour for Xanthan gum aqueous solution as the dispersed phase, and Newtonian canola oil as the continuous phase. Simulations were performed in OpenFOAM, using the interFoam solver and volume of fluid (VOF) method [3].

A cross-junction geometry with each inlet and outlet channel height (H) and width (W) equal to 50 micrometer with slight contractions in the conjunctions was used to gain a better monodispersity. Following validation of the numerical setup, we conducted a series of tests to provide novel insight into this configuration.

With Capillary number $(Ca = \mu_c U_c/\sigma)$, of 0.01, dispersed phase to continuous phase flow-rate ratio of 0.05, and contact angle of 160°, simulations revealed that by increasing the Xanthan gum concentration (0, 800, 1500, 2500 ppm) or in other words, decreasing the n -flow behaviour index- from 1 to 0.491, 0.389, and 0.302 in power-law model [4] : (a) breakup of the dispersed phase thread occurred at 0.0365, 0.0430, 0.0440, 0.0450 s; (b) the dimensionless width of the thread (W_{thread}/W) at the main channel entrance increased from 0 to 0.066, 0.096, 0.16; and (c) the dimensionless droplet diameter $(D_{droplet}/W)$ decreased from 0.76 to 0.72, 0.68, 0.67, respectively. Our next plan is to study effect of shear-thinning behaviour on droplet generation in different Ca and flow-rate ratios.

Keywords: droplet microfluidics; non-Newtonian fluid; volume of fluid

High-throughput Screening

Traditional biomedical tests are:

- being laborious
- time-consuming
- expensive
- in need of experienced operator

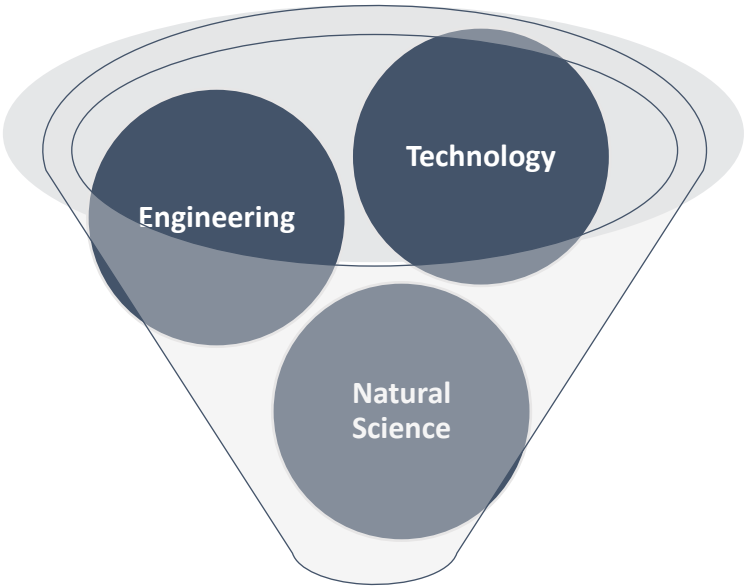

High-throughput screening (HTS) has been developed which refers to scientific experimental methods allowing rapid conduction of series of chemical and biological tests.

Biomedical Technology

prediction, diagnosis, and treatment of various inherited and acquired illnesses.

Microfluidic Technology

❖ Microfluidics is becoming a preferred choice for research and diagnosis due to two main reasons:

I. low sample/ reagent consumption and high processing speed

II. extreme flow confinement (Re < 1) ➡ high control over the fluid molecules in space and time

❖ Droplet-based microfluidics

an intriguing subject with promising future

enables control over:

- volume
- frequency
- composition

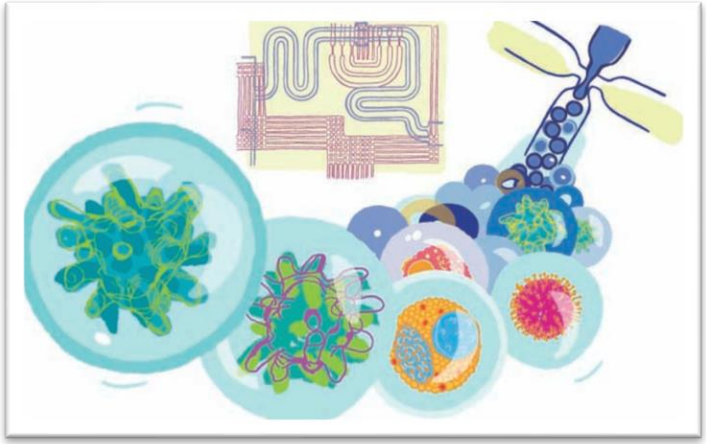

Fig 1- Droplet microfluidics
(Taken from https://www.kth.se/pro/nanobio/droplet-microfluidics-1.366373)

Microfluidic CFD

Many researches have used CFD tools to investigate the microfluidic devices behaviour including droplet generation in different regimes and novel geometries.

Computational fluid dynamics (CFD) can investigate

- influence of different physical parameters
- their relations to generated droplets size/ frequency
- in a less expensive systematically manner.

Yet, there are some aspects in need of further investigation so that the CFD results would become more reliable and accurate.

Aim of Research

Aim: *Generating series of non-Newtonian isolated droplets for high-throughput screening*

Justification:

- Many biological/chemical solutions used in biotechnology → shear thinning non-Newtonian
- Most studies consider Newtonian fluids
- To improve the reliability of simulation results in real-life assays

Governing Equations

Volume of Fluid (VOF) ⟶ Navier-Stokes equations for both fluids is combined with advection equation for the fluid fraction α

$$\nabla . \boldsymbol{U} = 0 \qquad \text{(Equation 1)}$$

$$\rho\left(\frac{\partial \boldsymbol{U}}{\partial t} + \boldsymbol{U}.\nabla \boldsymbol{U}\right) = -\nabla P + \rho \mathbf{g} + \nabla . \mu(\nabla \mathbf{U} + \nabla \mathbf{U}^T) + F_s \qquad \text{(Equation 2)}$$

VOF

$$\frac{\partial \alpha}{\partial t} + \nabla . (\mathbf{U}\alpha) = 0 \qquad \text{(Equation 3)}$$

$$\rho = \rho_1 \alpha + \rho_2 (1 - \alpha) \qquad \text{(Equation 4)}$$

$$\mu = \mu_1 \alpha + \mu_2 (1 - \alpha) \qquad \text{(Equation 5)}$$

Power-law Fluid: $\mu(\gamma) = K\gamma^{n-1}$ (Equation 6)

Software:

- OpenFOAM 8
  - Free, open source CFD software developed primarily by OpenCFD Ltd since 2004.
- Solver : interFoam
  - Solver for 2 incompressible, isothermal immiscible fluids using a VOF
- Multidimensional universal limiter with explicit solution (MULES) algorithm to solve the advection equation for the volume fraction

Numerical Settings

- Pressure-velocity coupling: PISO scheme
- Transient terms discretised scheme: first order implicit Euler
- Interpolation scheme: linear
- Spatial discretisation scheme: combination of second order upwind and central differencing with the van Leer limiter
- Maximum Courant number: 0.5
- Maximum Courant number of the interface: 0.25

$$\mathrm{Co} = \mathrm{U}\frac{\Delta t}{\Delta X}$$

Material:

- Dispersed phase: Xanthan gum aqueous solution
  - non-Newtonian power-law fluid
- Continuous phase: canola oil (Newtonian fluid)

Table 1- Properties of the liquids and parameters of the power-law fit of the xanthan solutions [4]

Fluid	Viscosity [Pa.s]	Density [kg/m^3]	n	K [Pa.s^n]
water	0.00089	997	-	-
oil	0.0223	930	-	-
800 ppm (w/w) xanthan/ water	0.076	997	0.491	0.0755
1500 ppm (w/w) xanthan/ water	0.312	997	0.389	0.3125
2500 ppm (w/w) xanthan/ water	0.985	997	0.302	0.985

Geometry specification:

- W= 50 μm
- Slope of contraction/expansion = 1/5

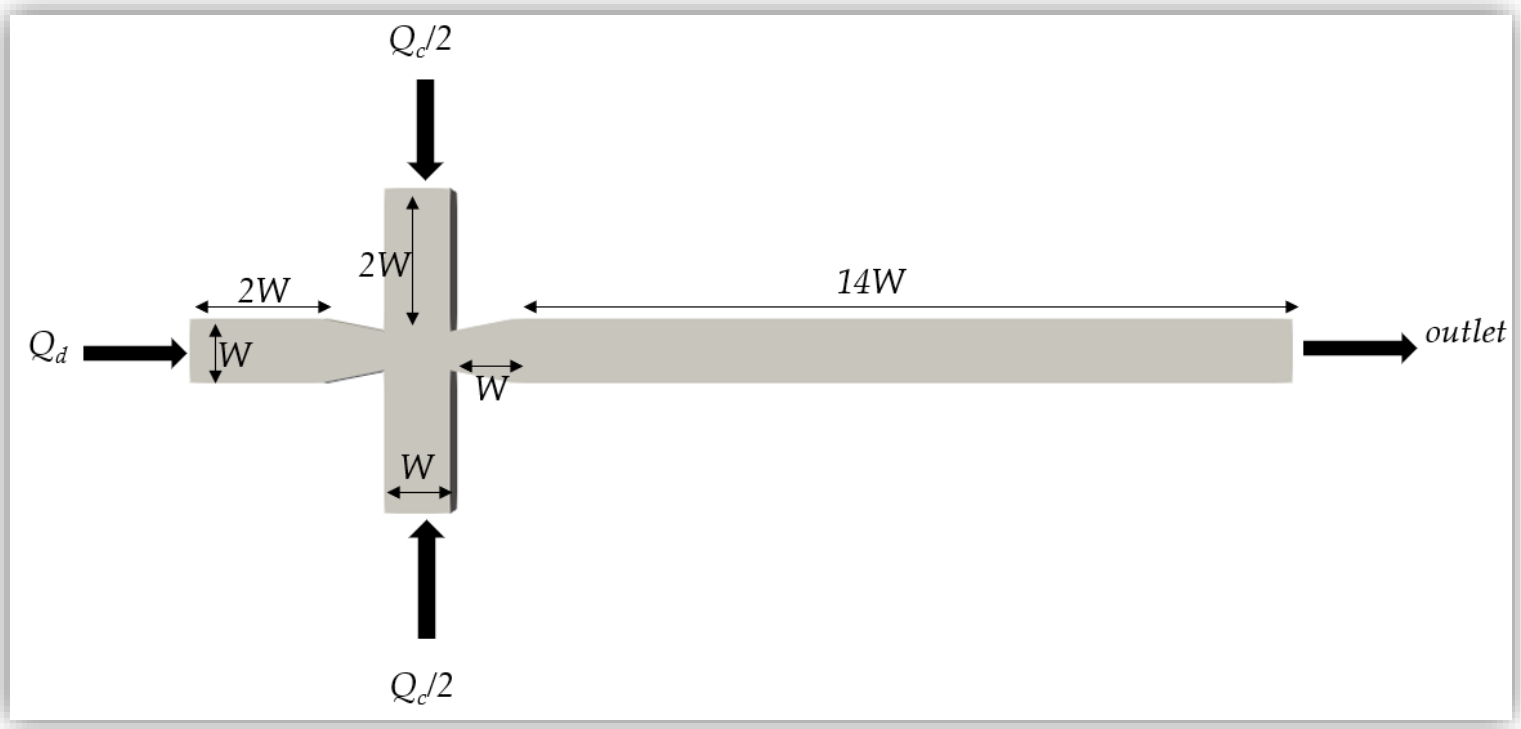

Fig 2 - Geometry of studied cross-junction

Mesh

Mesh was generated using “blockMesh”

- Structured mesh
- Different mesh size were studied 25 , 50, 75, 100 per 100 microns
- Optimum: 50 cells per 100 microns ⟶ accurate results as well as sharp interface

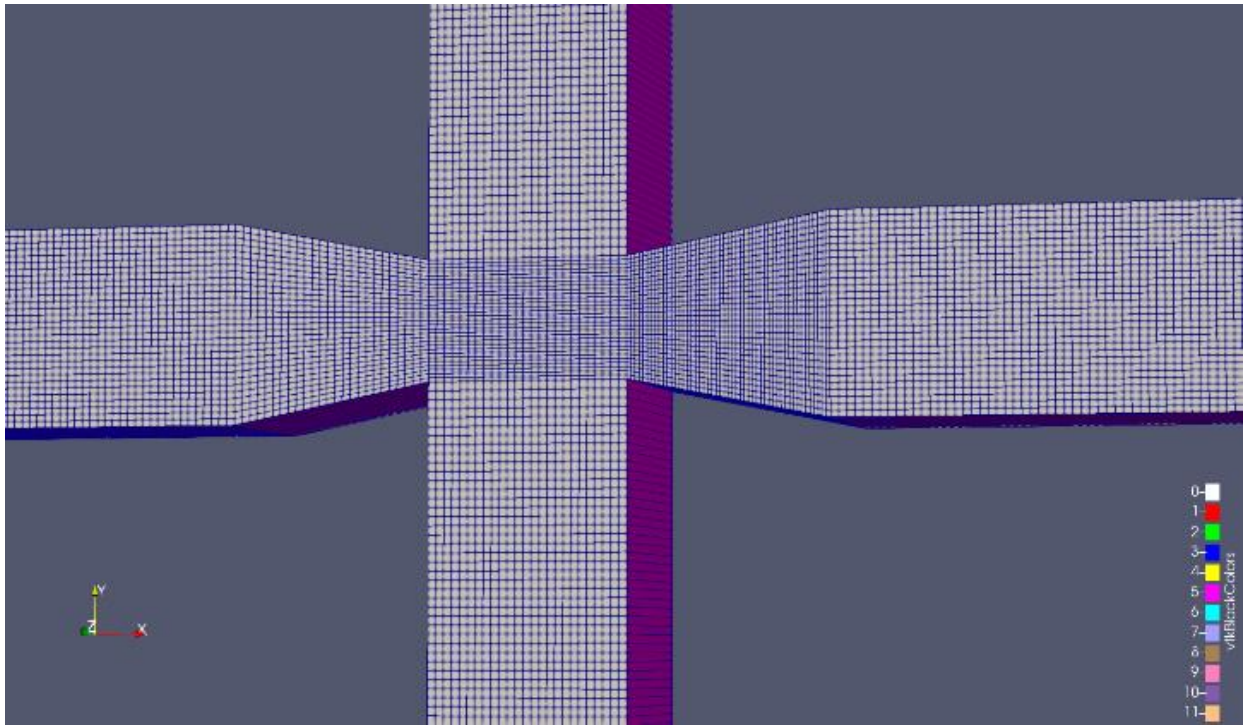

Fig 3 - Meshed geometry

The results were validated against Wu et al. [6] and error was less than 7% in all studied cases.

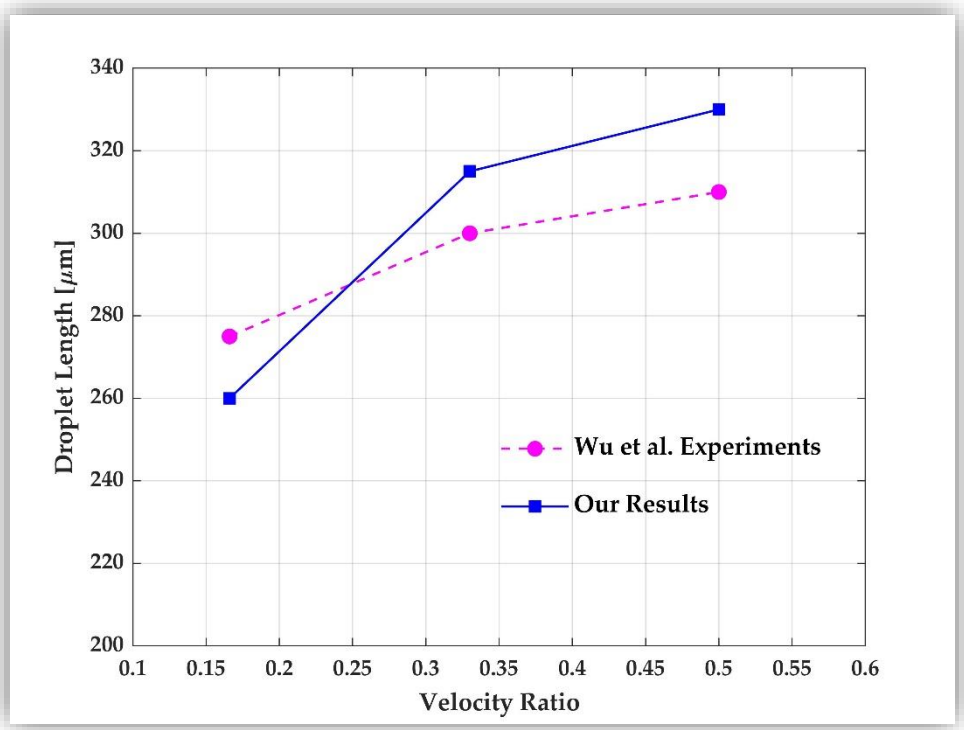

Figure 4 - Droplet length results compared against the experimental results of Wu et al. [6] for $U_o = 0.00252$ (m/s) , $\sigma = 30$ (mN/m), and $\mu_o / \mu_w = 0.416$

Results

In the simulations:

- the capillary number and flow rate ratio were kept constant:

$$Ca = \frac{\mu_c U_c}{\sigma} = 0.01\ ; \quad \frac{Q_d}{Q_d} = 0.05\ ; \quad \text{contact angle} = 160^{\circ}$$

- while the concentration of polymer and thus, the power-law index was changed.

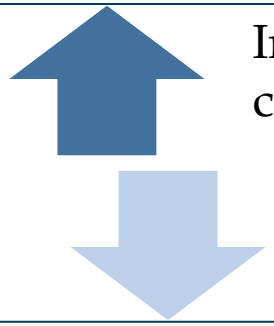

Increasing the Xanthan gum concentration (0, 800, 1500, 2500 [ppm])

Decreasing the n from 1 to 0.491, 0.389, and 0.302 in power-law model

Three effects were studied:

A. Droplet detachment time
B. Thread width
C. Droplet diameter

A. Effect on Droplet Detachment Time

❖ Breakup of the dispersed phase thread experienced a delay by up to 23%.

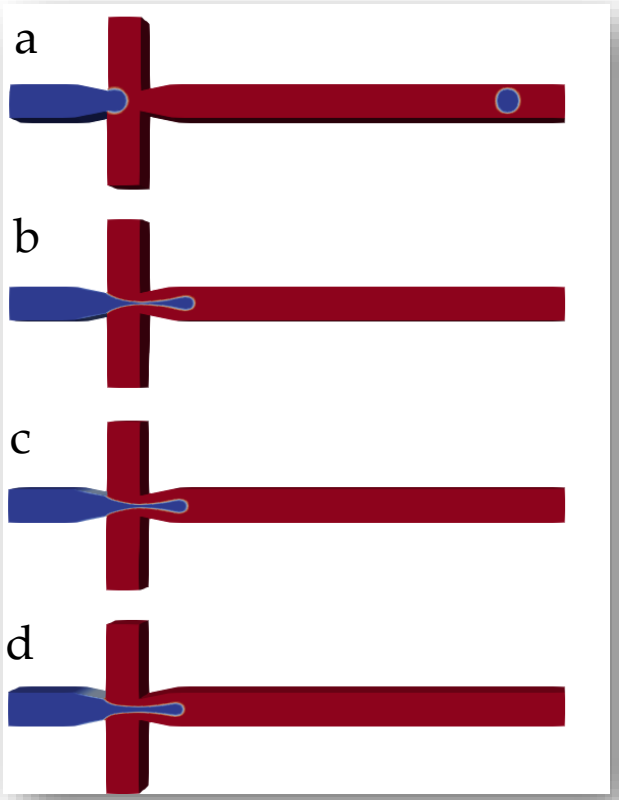

Fig 5 – Effect of increasing the polymer concentration on droplet formation

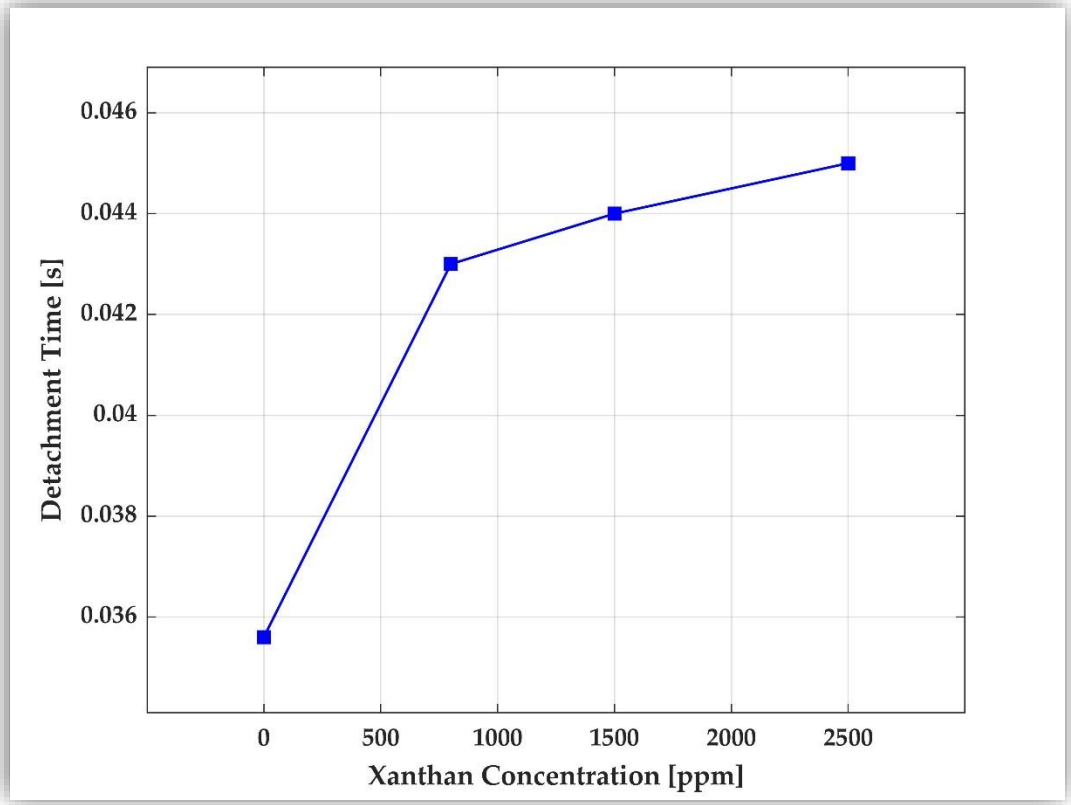

Fig 6 – Effect of the polymer concentration on droplet detachment time

B. Effect on Thread Width

- Dimensionless width of the thread ($\frac{W_{thread}}{W}$) at the main channel entrance increased from 0 to 0.066, 0.096, 0.16.

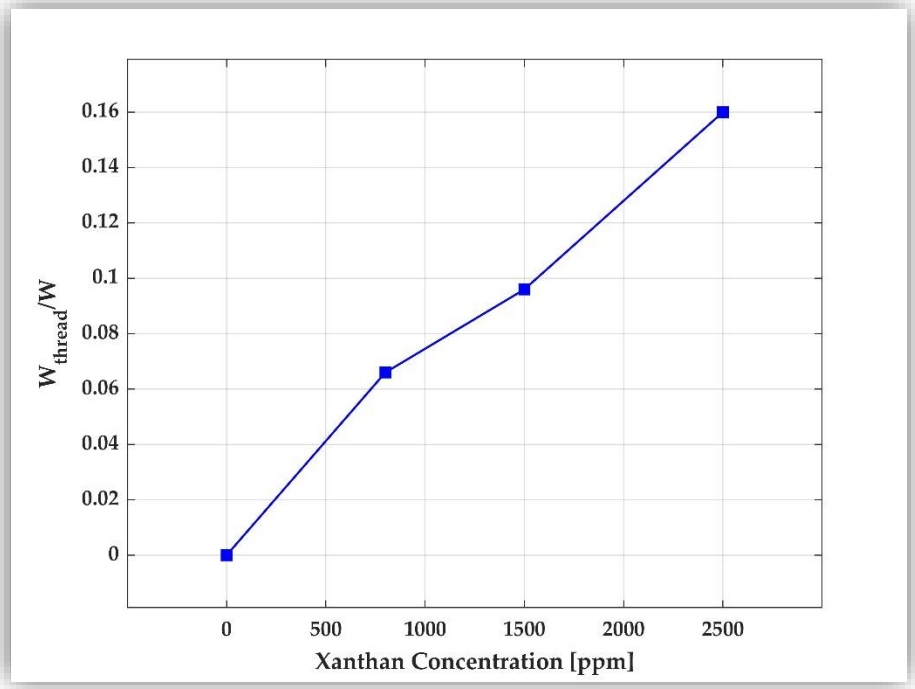

Fig 7 – Effect of the polymer concentration on thread width

C. Effect on Droplet Diameter

- Dimensionless droplet diameter ($\frac{D_{droplet}}{W}$) decreased from 0.76 to 0.72, 0.68, 0.67.

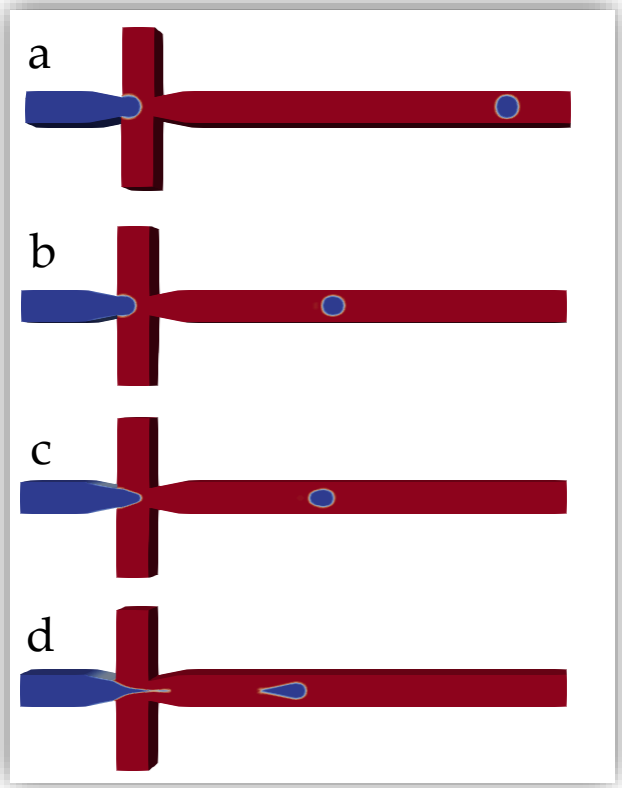

Fig 8 – Effect of increasing the xanthan concentration from a) 0, b) 800, c) 1500 d) 2500 [ppm] on droplet formation

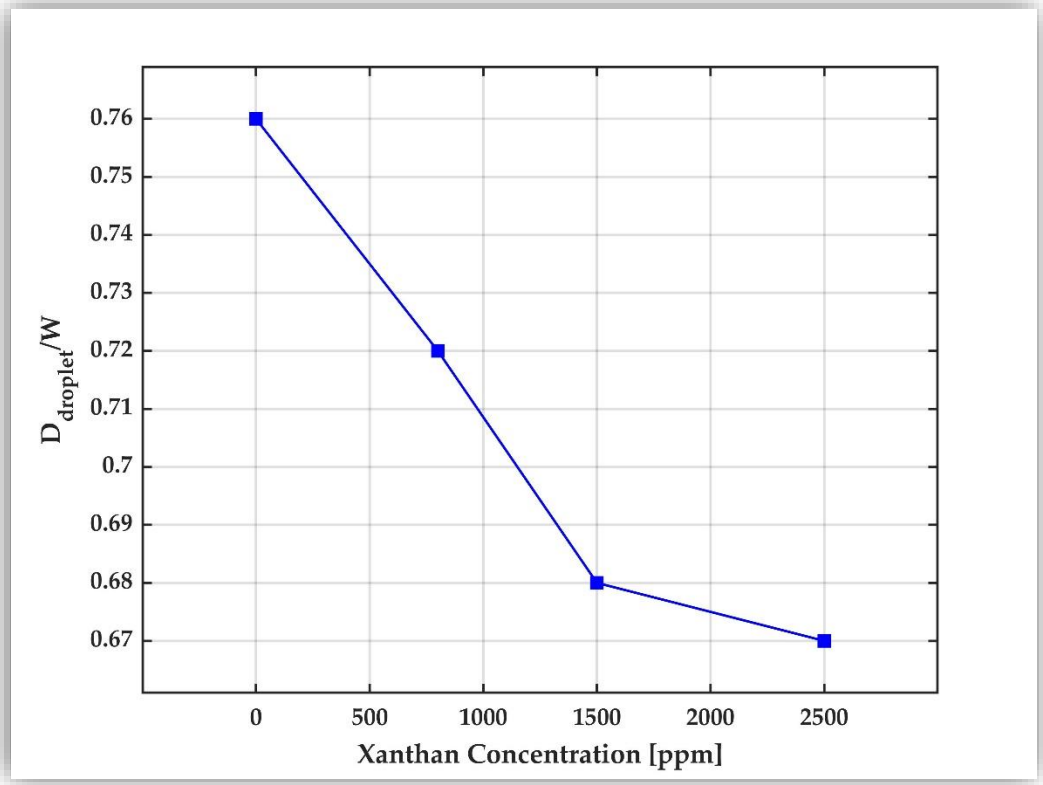

Fig 9 – Effect of the polymer concentration on droplet diameter

Conclusion

Many studies that use CFD tools to investigate droplet generation, focus on Newtonian fluids only. As most of solutions used in biological tests are non-Newtonian, this gap was addressed in this research.

By considering non-Newtonian power-law fluid as dispersed phase and simulating the droplet generation using VOF in OpenFOAM 8 software , the following was achieved.

By increasing the polymer concentration:

1. Droplet detachment time is increased between 18% to 23%.
2. Necking started to occur and increased respectively.
3. Dimensionless droplet diameter ($\frac{D_{droplet}}{W}$) decreased between 5.5% to 12%.

References

1. Eun, Y. J., Utada, A. S., Copeland, M. F., Takeuchi, S., & Weibel, D. B. (2011). Encapsulating bacteria in agarose microparticles using microfluidics for high-throughput cell analysis and isolation. ACS chemical biology, 6(3), 260-266
2. Khater, A., Abdelrehim, O., Mohammadi, M., Azarmanesh, M., Janmaleki, M., Salahandish, R., ... & Sanati-Nezhad, A. (2020). Picoliter agar droplet breakup in microfluidics meets microbiology application: numerical and experimental approaches. Lab on a Chip, 20(12), 2175-2187.
3. Chen, Q., Li, J., Song, Y., Christopher, D. M., & Li, X. (2020). Modeling of Newtonian droplet formation in power-law non-Newtonian fluids in a flow-focusing device. Heat and Mass Transfer, 56(9), 2711-2723.
4. Taassob, A., Manshadi, M. K. D., Bordbar, A., & Kamali, R. (2017). Monodisperse non-Newtonian micro-droplet generation in a co-flow device. Journal of the Brazilian Society of Mechanical Sciences and Engineering, 39(6), 2013-2021.
5. Sontti, S. G., & Atta, A. (2019). Numerical insights on controlled droplet formation in a microfluidic flow-focusing device. Industrial & Engineering Chemistry Research, 59(9), 3702-3716.
6. Wu, L., Tsutahara, M., Kim, L. S., & Ha, M. (2008). Three-dimensional lattice Boltzmann simulations of droplet formation in a cross-junction microchannel. International journal of multiphase flow, 34(9), 852-864.
7. Soh, G. Y., Yeoh, G. H., & Timchenko, V. (2016). Improved volume-of-fluid (VOF) model for predictions of velocity fields and droplet lengths in microchannels. Flow Measurement and Instrumentation, 51, 105-115.

Thank you for your attention

Any questions?